



Cite this: *Polym. Chem.*, 2021, **12**, 2175

Synthesis and characterization of a pH-responsive mesalazine-polynorbornene supramolecular assembly†

Vajk Farkas, ^a Gábor Turczel, ^a János Deme, ^a Attila Domján, ^{a,b} László Trif, ^a Anvar Mirzaei, ^a Dang Vu Hai, ^a Márton Nagyházi, ^{a,c} Sándor Kéki, ^d Péter Huszthy ^c and Róbert Tuba ^a

A pH-responsive mesalazine–crown ether and perfluoro *tert*-butyl functionalized polynorbornene supramolecular assembly (**smc-1-4-cp-1-5**) has been prepared. A promoted mesalazine (**1**) anti-inflammatory drug sustained release has been observed at elevated pH (7–9) enabling targeted topical and sustained drug dosing in the inflamed lower gastrointestinal (GI) tract. Thermoanalytical and solid-state NMR investigations of the supramolecular assembly revealed an amorphous, solid solvent structure showing that **1** is evenly distributed in the supramolecular polymer framework. *In situ* ¹H NMR investigation revealed a downshift of the respective hydrogens upon mesalazine–supramolecular polymer assembly formation. The equilibrium constant of the complex of crown ether-functionalized norbornene monomer (**5**) and **1** ($\log K = 3.4 \pm 0.5$, in a DMSO-*d*₆–CD₂Cl₂ 1:1 mixture) was calculated.

Received 12th February 2021,
Accepted 4th March 2021

DOI: 10.1039/d1py00194a

rsc.li/polymers

Introduction

Mesalazine (**1**, 5-aminosalicylic acid, 5-ASA) is a highly potent anti-inflammatory drug to treat ulcerative colitis or Crohn's disease.¹ It is generally accepted that **1** exerts its effect in the gut lumen *via* topical actions.¹ **1** is a potent scavenger of reactive oxygen species, which are supposed to play a significant role in the pathogenesis.² Once orally administered, its absorption is most extensive in the proximal small bowel. Although several alternative oral dosage formulations have been developed to facilitate the delivery of **1** to more distal sites of inflammation, its precisely targeted and sustained release remained challenging.³ For mesalazine administration, in general, three types of sustained-release approaches are considered: (1) diffusion-dependent prolonged-release;⁴ (2) colonic bacterial azoreduction;⁵ and (3) pH-dependent delayed-release.⁶

The average residence time of chyme and the pH are significantly higher in the duodenum, small and large intestine (16 hours to several days, pH: 7.0–8.5), than in the upper digestive system (four hours, pH: 1.5–4.0).⁷ One of the most obvious approaches to design drug carrier molecules⁸ for targeted and sustained release of **1** is to seize the opportunity arising from the pH differences of the gastrointestinal tracts. The pH differences can be even more pronounced if there is inflammation in the intestinal tract.⁹

Polynorbornenes synthesized by ring-opening metathesis have become an emerging class of drug carrier polymers. Polynorbornenes have been demonstrated to be non-toxic in a variety of systems including mammalian cells.^{10–12} Although polynorbornenes cannot be considered as typical biodegradable polymers, their application as biocompatible drug delivery materials is known.^{13–16} Moreover, pH-responsive polynorbornene drug carrier macromolecules and biodegradable polynorbornene for biomedical applications have also been reported.^{17,18} The synthesis of several functionalized norbornene copolymers having pyridino-18-crown-6 ether, hydroxy and perfluoro-*tert*-butyl units by ruthenium-catalyzed ring-opening metathesis polymerization (ROMP) has recently been reported.¹⁹ It was demonstrated that the complexation of these copolymers with biogenic amines including dopamine (**2**) and L-alanyl-L-lysine dipeptide (**3**) led to the formation of the corresponding supramolecular assemblies.¹⁹

The equilibrium constant (K) values for the supramolecular complexes of crown ethers with aliphatic protonated primary

^aInstitute of Materials and Environmental Chemistry, Research Centre for Natural Sciences, Magyar tudósok körútja 2., 1519 Budapest, P.O. Box 286, Hungary.
E-mail: tuba.robert@ttk.hu

^bNMR Laboratory, Research Centre for Natural Sciences, Magyar tudósok körútja 2, Budapest, 1117, Hungary

^cDepartment of Organic Chemistry and Technology, Budapest University of Technology and Economics, Szent Gellért tér 4, H-1111 Budapest, Hungary

^dDepartment of Applied Chemistry, University of Debrecen, Egyetem tér 1, H-4032 Debrecen, Hungary

† Electronic supplementary information (ESI) available. See DOI: 10.1039/d1py00194a



amines including dopamine ($\log K = 4.3$) are in general high, indicating that the equilibrium is shifted to the complex formation side.^{20–24} The complexation of **1** with 18-crown-6 ether, however, renders a significantly lower $\log K = 2.15$ value,² revealing a greater extent of dynamic behavior. Therefore, it was tentatively expected that a small increment of pH changes – affecting the $-\text{NH}_2/-\text{NH}_3^+$ equilibrium (ESI Fig. S17†) – should have a high influence on the equilibrium and thus the drug-releasing properties of the polymer supramolecular assembly. This unique feature prompted us to investigate the supramolecular assembly and pH responsive drug release properties of pyridino-18-crown-6 ether units containing fluorine-functionalized polynorbornene and mesalazine (**1**).

Results and discussion

The supramolecular assembly formation of the perfluoro-*tert*-butyl-functionalized polymer **4-cp-1-5** (Fig. 3) involving one crown ether and five perfluoro-*tert*-butyl units has not been investigated yet. However, this polymer might be a suitable choice as a model transporter, since the enriched perfluorotagged organic moieties are not only biocompatible, but also enable the *in vivo* monitoring of the carrier macromolecules by magnetic resonance imaging (MRI) techniques.²⁵

In this study, the synthesis, structural characterization and drug release properties of a perfluoro-*tert*-butyl-functionalized poly-norbornene–mesalazine supramolecular assembly are reported.

The preliminary investigation of the formation of the supramolecular assembly **smc-1-5** was carried out by the titration of monomer **5** with **1** using *in situ* ^1H NMR. The presence of the **smc-1-5** supramolecular assembly was manifested by the gradually increasing downfield shift of the respective aromatic signals of **5** (6.77 ppm) (Fig. 1). As the stoichiometric ratio has been achieved, further addition of **1** did not cause remarkable changes in chemical shifts. Based on the chemical shift changes, $\log K = 3.4 \pm 0.5$ was calculated (DMSO-*d*₆–CD₂Cl₂ 1:1 mixture), which is consistent with the K values reported for similar complexes (see the ESI†).²⁶

Electronic structure calculations using Gaussian 09 program package²⁷ were carried out to determine the lowest-energy conformers of **5** and its complexes formed with mesalazine (**1**) at the M06-2X/cc-pVDZ level of density functional theory (DFT)^{28,29} using an SMD implicit solvent model.³⁰ Coordinates of optimized geometries are listed in the ESI.† The one with the lowest energy is shown in Fig. 2. Driven by secondary interactions, the macroring of the crown ether shrinks and folds back over the pyridine moiety.¹⁹ Upon complexation, however, the macroring of the crown ether folds out and takes a conformation, which can host the primary ammonium ion. Complexation of **1** proceeds by forming three H-bonds (distributed at every $\sim 120^\circ$) with the crown ether by two possibly different ways: either involving the nitrogen atom of the pyridine ring or without it. Based on the calculations the former is the energetically favored structure.

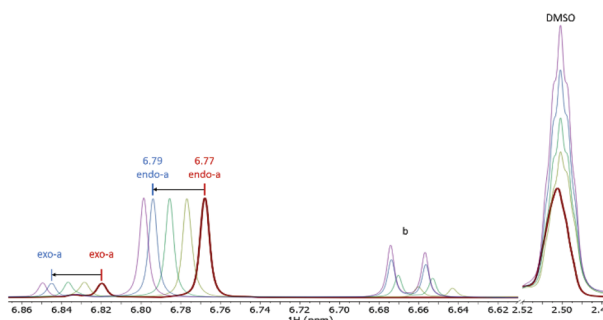
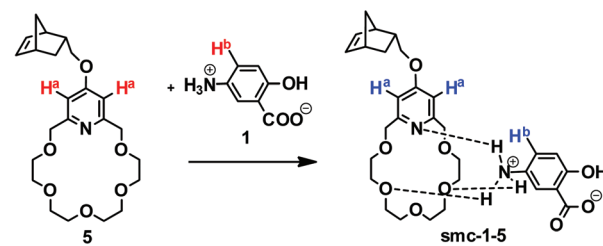


Fig. 1 Investigation of the complexation of **5** (*endo/exo* mixture) with **1** by titration ^1H NMR. Stoichiometric ratios: red: 0; yellow: 0.3; green: 0.6; light blue: 1.0; purple: 1.3 equivalents (DMSO-*d*₆–CD₂Cl₂ 1:1 mixture, $[5] = [1] = 0.06 \text{ mmol mL}^{-1}$).

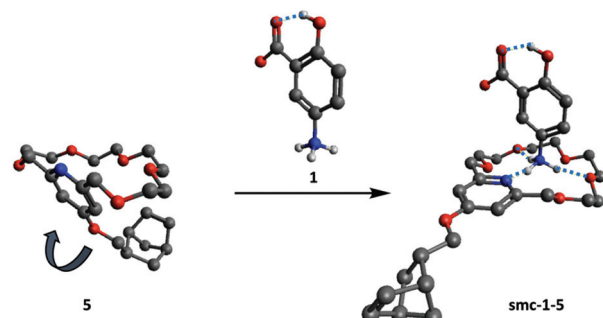


Fig. 2 DFT optimized minimum energy conformer of pyridino-18-crown-6 ether (**5**, left). DFT optimized low energy conformer of complex **smc-1-5** (right) in implicit water solvent.

The supramolecular complexation of polymer **4-cp-1-5** with **1** was investigated by ^1H NMR spectroscopy (Fig. 3). As expected, upon complexation the broad aromatic proton signals of **4-cp-1-5** shifted downfield from 6.50 to 6.55 ppm, meanwhile the aromatic protons of **1** also showed a significant downshift from 6.89 (d), 6.60 (dd) and 6.43 (d) ppm to 7.02 (d), 6.71 (dd) and 6.52 (d) ppm, respectively (Fig. 3). These observations are in accordance with the literature data reported for the supramolecular complex formation of pyridino-18-crown-6 ethers with protonated primary amines.²⁰ A chemical shift could also be observed in the case of the benzylic proton region of the crown ether as well. The benzylic CH₂ proton signals of **4-cp-1-5** (H^e) shifted from 4.32 and 4.23 ppm to 4.37 and 4.27 ppm, respectively. Interestingly, the



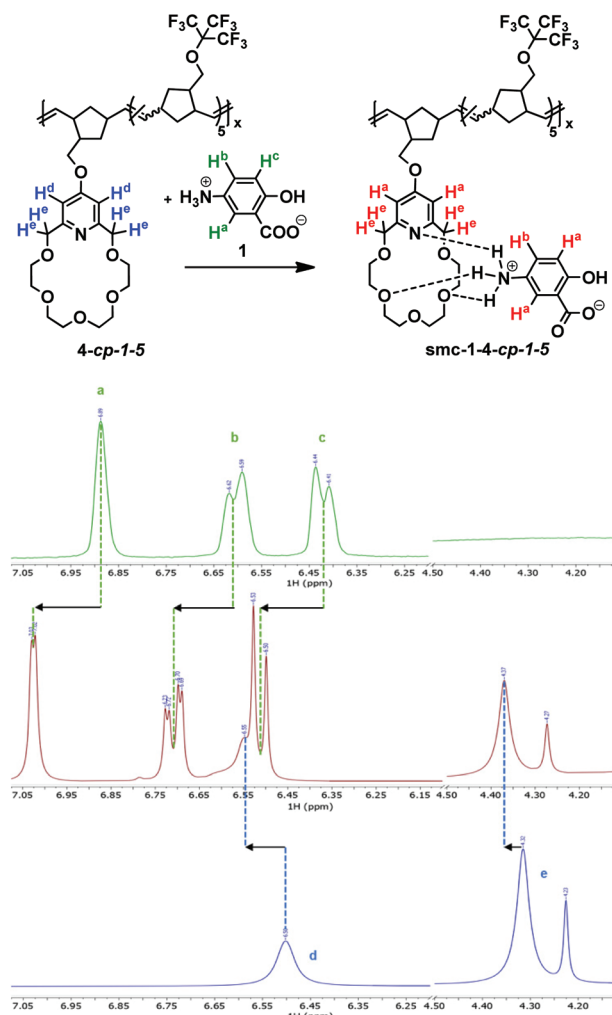


Fig. 3 Complexation of **4-cp-1-5** (bottom) with one equivalent of mesalazine (**1**, top) based on the crown ether moiety and **smc-1-4-cp-1-5** complex (middle) (DMSO- d_6 -CD₂Cl₂ 1:1 mixture, 30 °C, [1] = 0.06 mmol mL⁻¹).

proton signals of **1** showed relatively broad signals presumably due to the presence of zwitterionic **1** oligomers; however, upon complexation, the signals became narrower, indicating that the formed polymer supramolecular assembly contains disjointed, single mesalazine (**1**) units. Upon complexation the white color of the polymer turned purple immediately. Although polymer **4-cp-1-5** is soluble in CH₂Cl₂ and THF, the isolated supramolecular polymer **smc-1-4-cp-1-5** is poorly soluble in any common organic solvents. DMSO-CH₂Cl₂ was the only solvent mixture which sparingly dissolved the supramolecular complex making possible its ¹H NMR analysis. As was expected, the ¹⁹F NMR spectrum of the supramolecular polymer showed a peak at -70.64 ppm, which is very close to the chemical shift of **4-cp-1-5** (-70.59 ppm), indicating a significant distance between the perfluorinated and crown ether units of the polymer.

GPC analysis of **4-cp-1-5** indicated a 10.6 kDa average molecular weight (which concurred with the earlier reported

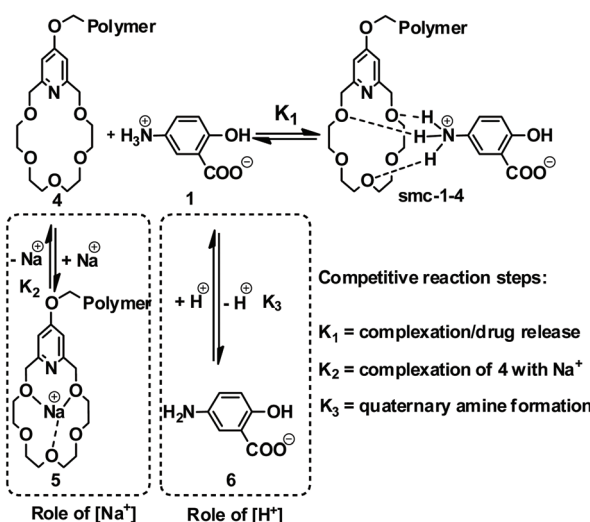
data);¹⁹ however, its supramolecular assembly was either non-soluble in THF or, due to its ionic character, it physically adsorbed on the column and showed a significantly longer elution time. The MALDI-TOF analysis confirmed the presence of **smc-1-4-cp-1-5** containing a single mesalazine molecule (Fig. S9†). However, supposedly due to the relatively weak interaction between **1** and **4-cp-1-5**, supramolecular **smc-1-4-cp-1-5** with two or more mesalazine molecules could not be detected under our MALDI conditions. Solid-state NMR characterization of the supramolecular complex **smc-1-4-cp-1-5** indicated an amorphous structure of the molecular assembly (see Fig. S6†). Narrow Lorentzian signals of crystalline mezalazin disappear in the spectrum of the assembly. Analysis of cross polarization curves is a powerful method to investigate matrix-drug interactions in the solid state.^{31,32} Cross polarization buildup curves show changes in the behavior of both the crown ether (Fig. S7†) and backbone (Fig. S8†) signals, as well. The buildup curve of crown ether groups rises faster because of the increased number of hydrogens in the neighborhood of the rings owing to complexation. Relaxation of backbone signals changes also by the effect of adduct formation which confirms that mezalazin molecules are evenly distributed in the matrix affecting the backbone. We can conclude that the formed mesalazine–polymer adduct is rather a solid solution than a solid dispersion, which is in agreement with the formation of the **smc-1-4-cp-1-5** supramolecular assembly. The presence and even distribution of **1** in **smc-1-4-cp-1-5** were also confirmed by thermal analysis. On the TG-DSC trace of **1** (see Fig. S13† in the ESI†), a sharp endotherm peak accompanied by substantial mass loss can be observed between 225 and 305 °C, which is the result of the melting and simultaneous chemical degradation of crystalline **1**. The calorimetric melting point of **1** (283.7 °C) is also in good agreement with the values in the literature (275–282 °C). The thermal analysis of **smc-1-4-cp-1-5** revealed the presence and even distribution of **1** in the supramolecular complex, which is confirmed by a small mass loss step (TG), and a small endotherm peak (DSC). It corresponds to the chemical degradation of **1** (see Fig. S13 and S15† in the ESI†). Based on the comparison of both mass loss values and the melting/degradation enthalpy values (between 205 and 295 °C) of **1**, the shifting of the small endotherm peak towards lower temperature (260.5 °C) also supports the uniform and even distribution of **1** in **smc-1-4-cp-1-5**. The content of **1** was found to be around 7% (more precisely, content of **1** determined from the mass loss step is 7.4 ± 0.2%, while the mesalazine content calculated from the melting/degradation enthalpy ratio is 7.6 ± 0.1%), which is in good agreement with the values determined from the dissolution measurements.

Mesalazine release of the **smc-1-4-cp-1-5** supramolecular assembly

Mesalazine (**1**) release tests using the **smc-1-4-cp-1-5** supramolecular polymer were carried out in aqueous phosphate buffer solution at preadjusted pH and aqueous sodium chloride concentration at 37 °C. The effect of pH was investigated in a 2.0–9.2 pH range, meanwhile the influence of sodium chloride



concentration on the sustained release was studied in a 0.06–0.60 M concentration interval. Tentatively it was expected that the pH affects the concentration of the primary ammonium salt (R-NH_3^+), meanwhile the sodium cation concentration has an influence on the equilibrium of the formation of the supramolecular complex. Actually, a competition between the R-NH_3^+ and sodium cation in the complex forming reaction step is expected (Scheme 1). As it has been mentioned earlier, the pH and the average residence time of chyme are significantly higher in the lower digestive system than in the upper gastrointestinal tract. As can be clearly seen in Fig. 4, only 7% of **1** is released after eight hours at pH 4.0 and even less at pH 2.0 (5%). However, as the pH was raised to 7.0 and later on to 9.2, significantly higher release of **1** was



Scheme 1 Competitive reactions (including Na^+ complexation and pH dependent $-\text{NH}_3^+/\text{-NH}_2$ shift) in the equilibrium of smc-1-4 complex formation.

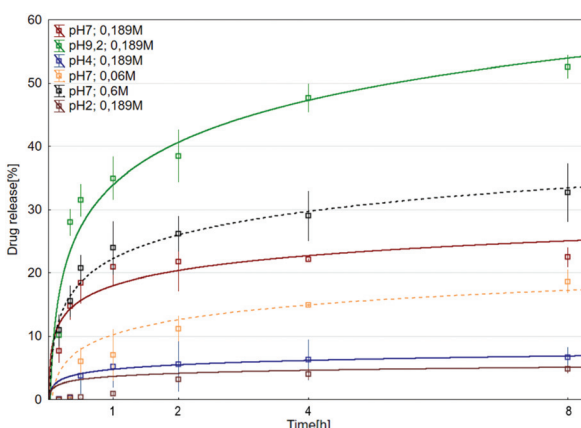


Fig. 4 Rate of mesalazine release from smc-1-4-cp-1-5 as a function of pH 2.0 (brown), 4.0 (blue), 7.0 (marine) and 9.2 (green) and sodium ion concentrations of 0.06 M (dashed orange) and 0.60 M (dashed black) at pH 7.0. $T = 37^\circ\text{C}$.

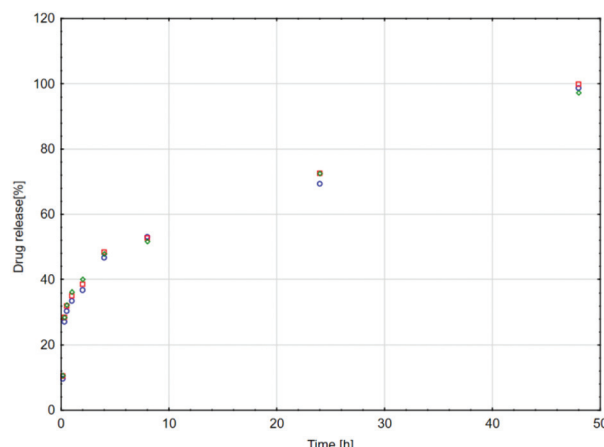


Fig. 5 Sustained mesalazine release from smc-1-4-cp-1-5 ($\text{pH} = 9.2$, $[\text{Na}^+] = 0.189$ M). $T = 37^\circ\text{C}$, $t = 48$ h (three independent runs).

observed (20% and 53%, respectively) at a similar time interval. At pH 9.2, complete drug release was observed within 48 h (Fig. 5). The effect of sodium ion concentration at pH 7.0 was also investigated. The experiments showed that higher sodium ion concentration caused faster release (Fig. 4, black dashed line). On the other hand, at lower sodium ion concentration, slower release (Fig. 4, yellow dashed line) could be observed.

$$C(t) = C_\infty [1 - e^{-(kt)^\lambda}] \quad (1)$$

It was found that the mesalazine release curves can be adequately described by a stretched exponential function (Weibull-function)³³ up to *ca.* 60% of release (eqn (1)), where C_∞ is the value (percentage) of the final (equilibrium) release ratio, and k and λ are the parameters describing the rate and distribution of the release. The parameters of the model were determined by fitting eqn (1) to the corresponding experimental release curves. According to the results, the values of λ were found to vary between 0.5 and 0.6 (only exception to that is the release curve at pH 7 and $[\text{Na}^+] = 0.189$ M). This finding may indicate Fickian diffusion of mesalazine.³⁴ The results of the fitting are summarized in the ESI (Fig. S18†).

However, it should also be considered that at low pH, pyridinium salt formation might occur initiating mesalazine release. Nevertheless, as the $\log K$ values of the reaction of pyridino-18-crown-6 ether with a proton ($\log K = 4.80$) and sodium ion ($\log K = 4.25$) are similar,^{35,36} when sodium ions are present competitive pyridine protonation and sodium ion complexation can take place. In our case however, the sodium ion concentration is twenty times higher than the proton concentration. Therefore, it is supposed that the formation of the pyridino-18-crown-6 ether-sodium complex is preferred to pyridine protonation.

Thus, it is assumed that the proton concentration may have limited impact on mesalazine release, since the sodium ion concentration is significantly higher above $\text{pH} = 2.0$. As the sodium complexation is presumably less affected by the



proton concentration under these conditions, it is supposed that the pH should have significant impact only on the mesalazine deprotonation but not on the pyridine protonation.

Conclusions

In summary, a pH-responsive mesalazine (**1**) supramolecular polymer assembly was synthesized. The solid NMR and thermoanalytical investigations of the synthesized **smc-1-4-cp-1-5** supramolecular assembly showed an amorphous, solid solvent structure. *In situ* ¹H NMR studies revealed downshifts of the concerned hydrogens. Upon titration of monomer **5** with **1**, $\log K = 3.4 \pm 0.5$ was calculated (in a DMSO-*d*₆-CD₂Cl₂ 1:1 mixture). The pH-dependent release of **1** was investigated at pH 2.0, 4.0, 7.0, and 9.2 showing enhanced release of mesalazine at elevated pH. The Na⁺ concentration was also found to have a significant impact on the release of **1**. At higher Na⁺ concentration faster mesalazine release was observed at pH 7.0. In conclusion, the reported supramolecular assembly-based drug delivery system demonstrated a targeted and sustained release of mesalazin (**1**) – a highly potent anti-inflammatory agent. This approach can open the door for innovative supramolecule based, pH responsive drug delivery systems.

Conflicts of interest

There are no conflicts to declare.

Acknowledgements

This work was funded by grants provided by the National Competitiveness and Excellence Program, Hungary (NVKP-16-1-2016-0007) and by the BIONANO-GINOP-2.3.2-15-2016-00017 project. We are grateful to Materia, Inc. for providing G2. Péter Huszthy is grateful to the National Research, Development and Innovation Office (NKFIH) for financial support under Grant No. K128473. Sándor Kéki is grateful to the Thematic Excellence Programme (TKP2020-IKA-04) of the Ministry for Innovation and Technology in Hungary, and Attila Domján is grateful to the Hungarian Scientific Research Fund (OTKA, K115939). We are grateful to Tibor Nagy for the helpful discussions and comments.

Notes and references

- 1 A. Tursi, C. Scarpignato, L. L. Strate, A. Lanas, W. Kruis, A. Lahat and S. Danese, *Nat. Rev. Dis. Primers*, 2020, **6**, 1–23.
- 2 A. A. Elbashir, F. A. A. Abdalla and H. Y. Aboul-Enein, *Luminescence*, 2015, **30**, 1250–1256.
- 3 B. Ye, *World J. Gastrointest. Pharmacol. Ther.*, 2015, **6**, 137.
- 4 D. Clemett and A. Markham, *Drugs*, 2000, **59**, 929–956.
- 5 N. Stojakovic, M. Mikov, S. Trbojevic, S. Vukmirovic, R. Skrbic and S. Satara, *J. Probiotics Health*, 2020, **8**, 6–13.
- 6 S. Matsumoto and Y. Yoshida, *Clin. Exp. Gastroenterol.*, 2015, **8**, 225–230.
- 7 S. G. Nugent, D. Kumar, D. S. Rampton and D. F. Evans, *Gut*, 2001, **48**, 571–577.
- 8 V. Taresco, C. Alexander, N. Singh and A. K. Pearce, *Adv. Ther.*, 2018, **1**, 1800030.
- 9 A. G. Press, I. A. Hauptmann, L. Hauptmann, B. Fuchs, M. Fuchs, K. Ewe and G. Ramadori, *Aliment. Pharmacol. Ther.*, 1998, **12**, 673–678.
- 10 E. M. Kolonko, J. K. Pontrello, S. L. Mangold and L. L. Kiessling, *J. Am. Chem. Soc.*, 2009, **131**, 7327–7333.
- 11 J. E. Gestwicki, L. E. Strong, C. W. Cairo, F. J. Boehm and L. L. Kiessling, *Chem. Biol.*, 2002, **9**, 163–169.
- 12 K. Lienkamp, A. E. Madkour, A. Musante, C. F. Nelson, K. Nüsslein and G. N. Tew, *J. Am. Chem. Soc.*, 2008, **130**, 9836–9843.
- 13 J. A. Johnson, Y. Y. Lu, A. O. Burts, Y. Xia, A. C. Durrell, D. A. Tirrell and R. H. Grubbs, *Macromolecules*, 2010, **43**, 10326–10335.
- 14 Y. Yu, H. Sun and C. Cheng, *Brush polymer-based nanostructures for drug delivery*, Elsevier Inc., 2017.
- 15 P. A. Bertin, K. J. Watson and S. B. T. Nguyen, *Macromolecules*, 2004, **37**, 8364–8372.
- 16 H. Maeda, J. Wu, T. Sawa, Y. Matsumura and K. Hori, *J. Controlled Release*, 2000, **65**, 271–284.
- 17 N. Vijayakameswara Rao, S. R. Mane, A. Kishore, J. Das Sarma and R. Shunmugam, *Biomacromolecules*, 2012, **13**, 221–230.
- 18 P. Shieh, H. V. T. Nguyen and J. A. Johnson, *Nat. Chem.*, 2019, **11**, 1124–1132.
- 19 E. Kovács, J. Deme, G. Turczel, T. Nagy, V. Farkas, L. Trif, S. Kéki, P. Huszthy and R. Tuba, *Polym. Chem.*, 2019, **10**, 5626–5634.
- 20 T. Wang, J. S. Bradshaw, J. C. Curtis, P. Huszthy and R. M. Izatt, *J. Inclusion Phenom. Mol. Recognit. Chem.*, 1993, **16**, 113–122.
- 21 T. Wang, J. S. Bradshaw and R. M. Izatt, *J. Heterocycl. Chem.*, 1994, **31**, 1097–1114.
- 22 C. Y. Zhu, J. S. Bradshaw, J. L. Oscarson and R. M. Izatt, *J. Inclusion Phenom. Mol. Recognit. Chem.*, 1992, **12**, 275–289.
- 23 J. S. Bradshaw, P. Huszthy, C. W. McDaniel, C. Y. Zhu, N. K. Dailey, R. M. Izatt and S. Lifson, *J. Org. Chem.*, 1990, **55**, 3129–3137.
- 24 S. V. Brignell and D. K. Smith, *New J. Chem.*, 2007, **31**, 1243–1249.
- 25 S. Decato, T. Bemis, E. Madsen and S. Mecozzi, *Polym. Chem.*, 2014, **5**, 6461–6471.
- 26 R. M. Izatt, T. Wang, J. K. Hathaway, X. X. Zhang, J. C. Curtis, J. S. Bradshaw, C. Y. Zhu and P. Huszthy, *J. Inclusion Phenom. Mol. Recognit. Chem.*, 1994, **17**, 157–175.
- 27 M. J. Frisch, G. W. Trucks, H. B. Schlegel, G. E. Scuseria, M. A. Robb, J. R. Cheeseman, G. Scalmani, V. Barone,



G. A. Petersson, H. Nakatsuji, X. Li, M. Caricato, A. V. Marenich, J. Bloino, B. G. Janesko, R. Gomperts and D. J. Fox, *Gaussian, 16, Revision C.01*, Gaussian, Inc., Wallingford CT, 2016.

28 Y. Zhao and D. G. Truhlar, *Theor. Chem. Acc.*, 2008, **120**, 215–241.

29 D. E. Woon and T. H. Dunning, *J. Chem. Phys.*, 1993, **98**, 1358–1371.

30 A. V. Marenich, C. J. Cramer and D. G. Truhlar, *J. Phys. Chem. B*, 2009, **113**, 6378–6396.

31 A. Domján, J. Bajdik and K. Pintye-Hódi, *Macromolecules*, 2009, **42**, 4667–4673.

32 A. Kazsoki, P. Szabó, A. Domján, A. Balázs, T. Bozó, M. Kellermayer, A. Farkas, D. Weiser-Balogh, B. Pinke and A. Darcsi, *Mol. Pharm.*, 2018, **15**, 4214–4225.

33 C. Mircioiu, V. Voicu, V. Anuta, A. Tudose, C. Celia, D. Paolino, M. Fresta, R. Sandulovici and I. Mircioiu, *Pharmaceutics*, 2019, **21**, 140–184.

34 V. Papadopoulou, K. Kosmidis, M. Vlachou and P. Macheras, *Int. J. Pharm.*, 2006, **309**, 44–50.

35 E. Rossini, A. D. Bochevarov and E. W. Knapp, *ACS Omega*, 2018, **3**, 1653–1662.

36 R. M. Izatt, K. Pawlak, J. S. Bradshaw and R. L. Bruening, *Chem. Rev.*, 1991, **91**, 1721–2085.

